Available online at www.sciencedirect.com
ScienceDirect
Chemical Engineering and Processing 46 (2007) 210–221
Chemical Engineering and Processing
www.elsevier.com/locate/cep

Degradation of the oxirane ring of epoxidized vegetable oils in a liquid–liquid–solid heterogeneous reaction system

Alejandrina Campanella, Miguel A. Baltanás *

INTEC, Instituto de Desarrollo Tecnológico para la Industria Química (Universidad Nacional del Litoral and Consejo Nacional de Investigaciones Científicas y Técnicas), Güemes 3450, S3000GLN Santa Fe, Argentina

Received 3 November 2005; received in revised form 6 April 2006; accepted 2 June 2006
Available online 9 June 2006

Abstract

The main oxirane-ring opening reactions that occur during the manufacture of epoxidized vegetable oils using a strongly acidic, gel-type ion exchange resin (IER) (Amberlite IR-120, 8% crosslinking) were analyzed. By using a heterogeneous liquid–liquid–solid model, the reactivity on each phase was individually assessed, taking into account each transport step as well as the relevant partition equilibria.

The combined results on the attack onto the oxirane ring of epoxidized vegetable oils by either hydrogen peroxide (H_2O_2) or solvated acetic acid (AA) indicate that under 'regular' process conditions these attacks proceed in the kinetic regime; that is, they are not mass-transfer controlled. The study indicated that most of the degradation occurs on the catalyst and, also, confirmed that the *external* surface protons of the IER are the main responsibles of the deleterious degradation of the oxirane ring as, in both cases, the degradation rate was directly proportional to the available external area of the catalyst.

Keywords: Oxirane ring opening; Liquid–liquid–solid reacting systems; Ion exchange resins

1. Introduction

Epoxidized vegetable oils are well established among the available plasticizers for manufacturing low cost, PVC-derived industrial items and household plasticware. Nowadays, they have also been recognized as an excellent intermediate towards the synthesis of biodegradable lubricants. The epoxidation of vegetable oils and/or their fatty acid methyl esters (FAME) with percarboxylic acids is the preferred route in industrial scale. Peracetic acid, prepared in situ using hydrogen peroxide (H_2O_2) as the primary source of oxygen and aqueous acetic acid (AA) as the oxygen carrier between the aqueous and the oil phases, is – most generally – the reactant of choice [1–5]. The process usually requires an acidic catalyst and although traditionally low cost mineral acids have been employed, they often hinder the achievement of high yields, owing to oxirane ring opening caused by deleterious consecutive reactions. The use of a heterogeneous catalyst capable of preventing the access of the oxirane group to the active catalytic sites has been, then, a strategy largely pursued.

In this regard, we recently began to study and evaluate (using a pseudohomogeneous model as a first step), the relative importance of each of the consecutive degradation reactions that occur during the epoxidation of soybean oil (SBO) with peracetic acid, when a sulfonic (strongly acidic), gel-type ion exchange resin (IER), such as Amberlite IR-120, is used [6,7]. This functionalized resin is hydrophilic, allowing only water, acetic acid and hydrogen peroxide into the gel phase; peracetic acid is produced inside and at the surface of the resin by sulfonic acid groups. Unlike macroreticular resin beads, the gel structure of IR-120 does not let large molecules such as triglycerides or FAME into the polymer network. Hence, a low oxirane-ring opening is expected as, in principle (and unlike with conventional heterogeneous catalysts), the acid-catalyzed oxirane degradation reactions can only occur on the external surface of the catalyst.

Then, the liquid–liquid–polymer catalyst system is truly heterogeneous: for the epoxide groups (Ep) to be degraded by the catalyst, they must cross the liquid–liquid interface as well as the liquid–solid interface (see Fig. 1). The occurrence of further, homogeneous degradation reactions makes the complete

* Corresponding author. Tel.: +54 342 455 9175; fax: +54 342 455 0944.
E-mail address: tderliq@ceride.gov.ar (M.A. Baltanás).

0255-2701/$ – see front matter © 2006 Elsevier B.V. All rights reserved.
doi:10.1016/j.cep.2006.06.001

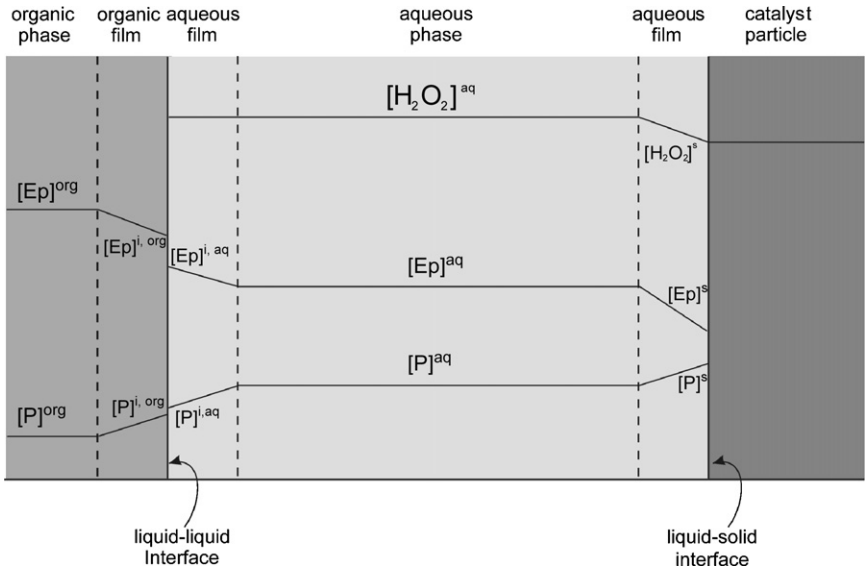

Fig. 1. Concentration profiles of the reactants and product in the liquid–liquid–solid reacting system under study, as exemplified by the degradation of the oxirane ring of epoxidized soybean oil by H_2O_2 (aq), using Amberlite IR 120 ion exchange resin (IER) as heterogeneous catalyst.

analyses somewhat more involved but, nevertheless, manageable. Thus, this work presents a detailed re-analysis on the case of two reactions occurring on these liquid–liquid–solid reacting system (the only truly relevant in the vegetable oil epoxidation process [8]): the opening of the oxirane ring with hydrogen peroxide and with solvated acetic acid, taking into account each of the transport and intrinsic kinetic steps in each phase. Separate series of experiments were conducted, using either aqueous H_2O_2 or solvated acetic acid.

2. Experimental

2.1. Materials

Crude soybean oil was refined (i.e., degummed, neutralized, bleached and deodorized) in the laboratory. Its fatty acid (FA) composition, as determined by GLC [9], was the following (wt.%): saturated FA (C16 + C18): 15.1, oleic acid: 21.5, linoleic acid: 55.7; linolenic acid: 7.7. The iodine value was 137.

Glacial acetic acid (acs, 99.8%), formic acid (acs, 99.8%), benzene (pa) and hydrogen peroxide (50 wt.%) were purchased from Fisher Scientific (Pittsburg, PA, USA). Heptadecanoic acid methyl ester (capillary CG, 99%) was purchased from Sigma-Aldrich (St. Louis, MO, USA). Amberlite IR-120 (Rohm & Haas), a strongly acidic, gel-type ion exchange resin with a DVB-styrene matrix and 8% crosslinking, functionalized with sulfonic groups, d_p(dry) = 215–775 μm (54.5% < 530 μm; 75.3% < 600 μm; 94.8% < 670 μm), was used throughout the work.

2.2. Preparation of epoxidized soybean oil (ESBO) stocks

The refined soybean oil was epoxidized in depth at low temperature (293–313 K) with performic acid generated in situ, using benzene as diluent of the organic phase, to minimize ring opening [5]. This procedure demands about 22 h to achieve reaction completion, though. The molar ratio of hydrogen peroxide/formic acid/SBO unsaturation (double bonds) was 20/2/1 and 500 ml of benzene per mol of double bond were added as well. The SBO, benzene and formic acid were jointly placed into a well-stirred, round-bottom glass reactor kept at 293 K. Then, dilute (30 wt.%) hydrogen peroxide (also at 293 K) was added dropwise, after which the reactor temperature was slowly raised to 313 K, to complete the reaction.

Two different ESBO stocks were prepared. The final content of epoxy oxygen in the first stock, used for the study of the degradation of the oxirane ring with hydrogen peroxide was 5.9 wt.%, while in the second ESBO stock (which was used to study the attack by solvated acetic acid) it was 5.5 wt.%. These figures are equivalent to a content of 0.36 and 0.34 kmol of oxygen/100 kg of ESBO, respectively. The final iodine values of said stocks were 3.6 and 2.2, respectively, while their final hydroxyl values were 0.1 and 0.5.

2.3. Determination of distribution constants

The distribution constants, or – more appropriately – the equilibrium molar ratios of the refined soybean oil and the ESBO in pure water and in aqueous solutions of hydrogen peroxide, were determined at 333–358 K, with and without H_2SO_4 added to the aqueous phase (pH 1).

On each test, 5 g of the soybean oil, or ESBO, were placed together with 20 g of water, or H_2O_2 (aq), in an erlenmeyer. The mixtures were equilibrated to the desired temperature, under constant stirring, during 4 h. Then, they were left to stand for at least 1 h until complete separation of the phases was achieved. Afterwards, an aliquot of the aqueous phase was carefully taken, using a syringe and a 0.2 μm teflon pre-filter. The determination of the distribution constants was done by measuring the amount of total organic carbon (TOC) in the aqueous phase,

Table 1
Distribution constants (equilibrium molar ratios) of soybean oil (m_{oil}) and epoxidized soybean oil (m_{Ep}) between the organic and the aqueous phases[a]

T (K)	$[H_2O_2]^{aq,o}$ (wt.%)	pH[b]	$m_{oil} \times 10^6$	$m_{Ep} \times 10^6$
333	0	N.A.[c]	1.19	1.58
	0	1	1.31	–
	30	N.A.	1.82	–
343	0	N.A.	1.43	2.09
	0	1	1.68	–
	15	N.A.	1.92	2.68
	15	1	1.97	–
	30	N.A.	2.09	2.76
	30	N.A.	2.68	–
	48	N.A.	3.21	–
353	0	N.A.	1.71	2.17
	0	1	1.98	–
	30	N.A.	3.38	–

[a] $m_j = [j]^{aq}/[j]^{org}$; j = soybean oil or epoxidized soybean oil; [j] = mol l^{-1}.
[b] By adding H_2SO_4 to the aqueous phase.
[c] No addition of mineral acid.

using a SHIMADZU model 5000 A TOC analyzer. The full set of experimental values is given in Table 1.

The distribution constant of ESBO cannot be determined when sulfuric acid is added to the system, because ESBO will react with the water or hydrogen peroxide [11]. However, as we can see in Table 1 the distribution constants of the refined soybean oil in pure water, with and without H_2SO_4 added to the aqueous phase, at the different temperatures, are fairly constant. So, for calculation purposes we assumed here that the distribution constant of ESBO with and without H_2SO_4 added are equal.

2.4. Activation and conditioning of the ion exchange resin

The IER was activated with hydrochloric acid (10 wt.%), in successive ion-exchange steps, with further washing using distilled demineralized water until complete elimination of the residual salinity. Then, glacial acetic acid (purity > 99.7 wt.%) was used to substitute water inside the resin.

The exchange capacity of IR-120, as determined by titration using conventional volumetric techniques, was: $[H^+]^\circ = 4.507$ eq kg^{-1} (dry basis). The dry polymer density was 1.437 kg m^{-3}. Three sieved fractions of the dry resin, with nominal diameters 50, 200 and 500 μm, were used to evaluate the possible impact of mass-transfer resistances, or protons availability (see below) on the process rate.

2.5. Oxirane ring opening studies

The stock of ESBO was used to study the opening of the oxirane ring caused by hydrogen peroxide and solvated AA (which is partitioned between the aqueous and the organic phases) in the presence of the strongly acidic, heterogeneous catalyst, Amberlite IR-120. Before using the activated IER for these studies, the material was preconditioned, i.e., washed several times with doubly distilled, deionized water until it was acid-free and then dried in an oven. For each run, aliquots of the preconditioned IER were mixed with the appropriate amount of either an aqueous solution of H_2O_2 (no acetic acid added in this case) or AA (no hydrogen peroxide added in this second case). The mixtures were placed into a 3-bore thermostatized round-bottom flask, furnished with a reflux condenser and a mechanical stirrer. The mixture was left to stand for 24 h and then the system was heated to work temperature. Next, a suitable volume of ESBO, previously thermostatized at the same temperature, was added to the reactor. Periodically, samples were taken and the IER was separated from the liquid phase. The aqueous phase was eliminated and the organic phase was then thoroughly washed to eliminate acidity and dried, using a rotary evaporator, prior to their derivatization and chemical analysis.

A molar excess of hydrogen peroxide or AA(aq) with respect to the epoxide groups was always used. The experimental program included several levels of temperature, hydrogen peroxide or AA concentration, IER amount and resin particle diameter, as detailed in Tables 2 and 3.

Table 2
Reaction conditions and conversion of epoxide oxygen in the organic phase in the acid-catalyzed opening of the oxirane ring of ESBO by H_2O_2(aq), using Amberlite IR 120 ion exchange resin as solid catalyst

Run[a]	T (K)	$[H_2O_2]^{eq,aq}$ (wt.%)[b]	Amount of IER (wt.%)[c]	IER particle diameter (μm)[d]	Total duration (min)	Final amount of epoxide oxygen (wt.%)[e]	Final percentage conversion[f]
1	333	33.35	2.83	634	1530	4.89	17.1
2	343	33.35	2.83	634	390	5.09	13.7
3	358	33.35	2.83	634	450	3.67	37.8
4	343	33.35	2.83	272	330	3.16	46.5
5	343	33.35	2.83	63	240	4.52	23.3
6	343	33.35	8.49	634	660	5.23	11.4
7	358	22.69	2.83	634	400	4.07	31.1
8	358	16.85	2.83	634	400	3.71	37.2

[a] Stirring rate = 1500 rpm.
[b] Obtained from Fig. 2.
[c] Weight percent of the ion exchange resin (IER) with respect to the mass of ESBO introduced in the reactor, dry basis.
[d] Water-swelled ion exchange resin particles [12].
[e] Final weight percent of epoxide oxygen of the oil in the organic phase ($\%EpO_{final}$). The full set of experimental data is given in Refs. [6–8].
[f] Percent conversion of epoxide oxygen, calculated as: $[(\%EpO_{initial} - \%EpO_{final})/\%EpO_{initial}] \times 100$, where $\%EpO_{initial}$ stands for the initial weight percent of epoxide oxygen (The $\%EpO_{initial}$ was 5.90).

Table 3
Reaction conditions and final weight percent of epoxide oxygen in the organic phase (conversion) in the acid-catalyzed opening of the oxirane ring of ESBO by water-solvated acetic acid, using Amberlite IR-120 ion exchange resin as solid catalyst

Run[a]	T (K)	$[AA]^{eq,aq}$ (kmol m^{-3})[b]	Amount of IER (wt.%)[c]	IER particle diameter (μm)[d]	Total duration (min)	Final amount of epoxide oxygen (wt.%)[e]	Final percentage conversion[f]
1	343	11.65	2.83	634	180	2.35	57.2
2	333	11.65	2.83	634	180	3.44	37.5
3	353	11.65	2.83	634	180	1.13	79.4
4	343	13.85	2.83	634	180	1.26	77.0
5	343	8.83	2.83	634	180	3.05	44.6
6	343	3.50	2.83	634	180	4.65	15.4
7	343	11.65	2.83	272	180	0.73	86.7
8	343	11.65	2.83	63	60	0.48	91.3
9	343	11.65	8.49	634	180	0.42	92.4

[a] Stirring rate = 1500 rpm.
[b] Obtained from Fig. 3 and employing densities of mixtures estimated from correlations given in [20]. For full details see also Ref. [8].
[c] Weight percent of the ion exchange resin (IER) with respect to the mass of ESBO introduced in the reactor, dry basis.
[d] Water-swelled ion exchange resin particles [12].
[e] Final weight percent of epoxide oxygen oil in the organic phase ($\%EpO_{final}$). The full set of experimental data is given in Refs. [6–8].
[f] Percent conversion of epoxide oxygen, calculated as: $[(\%EpO_{initial} - \%EpO_{final})/\%EpO_{initial}] \times 100$, where $\%EpO_{initial}$ stands for the initial weight percent of epoxide oxygen (The $\%EpO_{initial}$ was 5.50).

2.6. Analysis and data processing

Iodine and hydroxyl values of the stock of epoxidized soybean oil were analyzed using AOCS recommended practices [9]. The oxirane ring-opening reaction was followed by GLC [10], using a Shimadzu GC-17ATF unit furnished with a PE-5 capillary column: 30 mm × 0.53 mm i.d. × 1.5 μm film. Analytical conditions were as follows: split/splitless injector, injector port at 523 K, FID detector at 543 K, H_2 carrier gas (90 psig, 20 ml min^{-1}), and isothermal oven at 473 K. The response factors were obtained using heptadecanoic acid methyl ester as internal standard. Prior to injection, the dry samples were previously derivatized to FAME with sodium methoxide [10]. Each of the reported concentrations of epoxide groups in Tables 2 and 3 is the mean of three replicates; the coefficients of variation were always less than 9.5%. Standard deviations in the regression analyses are given for a 95% confidence interval.

3. Results and discussion

3.1. Oxirane ring-opening with hydrogen peroxide

Whenever a solid acidic catalyst is used, the opening of the oxirane ring cannot proceed in the aqueous phase (as the protons are confined into the catalyst particles). Besides, as it was already mentioned the degradation reaction can only proceed on the external surface of the catalyst particles, because the bulky molecules of the ESBO cannot enter the (gel-type) ion exchange resin [6]. In addition, it is timely to recall – for modeling purposes – that: (i) under typical process conditions the impact of hydrolysis is negligible [11]; (ii) hydrogen peroxide (which is insoluble in the organic phase) is always in excess in the media and (iii) the ESBO is the disperse phase in the reacting system. Fig. 1 depicts the system under study. Table 2 details the different experimental conditions under which the ring-opening with H_2O_2(aq), in the presence of Amberlite IR-120 was analyzed, and the final conversions after given elapsed times.

In the following we detail the mass balances for the reactive compound (the epoxide functional groups) in the different phases, considering the device as an ideal – i.e., perfectly mixed – isothermal batch reactor, and assuming that the total volume, as well as the individual volumes of each phase remain constant during the process (the density of ESBO is practically identical to that of the product of the ring-opening).

In the organic phase:

$$\frac{1}{V}\frac{dn_{Ep}^{org}}{dt} = -J_{Ep}^{org}a \quad (1)$$

where n_{Ep}^{org} is the number of moles of epoxide in the organic phase (which is equal to $[Ep]^{org}V_{org}$), J_{Ep}^{org} is the molar flux of Ep out of the organic phase (kmol m^{-2} s^{-1}), $[Ep]^{org}$ is the concentration of Ep in the bulk of the organic phase (kmol m^{-3}), a is the interfacial area between the organic and the aqueous phases (m^2 m$_{tot.}^{-3}$), V is the total liquid volume in the reactor (m$_{tot.}^3$) and V_{org} is the volume of the organic phase.

The organic–aqueous interface is at steady-state, so that:

$$aJ_{Ep}^{org} = aJ_{Ep}^{aq} \quad (2)$$

where J_{Ep}^{aq} is the incoming molar flux of Ep from the organic phase (kmol m^{-2} s^{-1}).

Likewise, considering steady-state in the aqueous phase (owing to the negligible accumulation of Ep and the absence of homogeneous chemical reaction):

$$aJ_{Ep}^{aq} - a_s J_{Ep}^{s} = 0 \quad (3)$$

where a_s is the liquid–solid interfacial area (m^2 m$_{tot.}^{-3}$).

Finally, taking into account that the mass flow of Ep through the liquid–solid interface is identical to its total rate of reaction on the external surface of the catalyst (using the steady-state approximation on the catalyst surface as well):

$$a_s J_{Ep}^{s} - R_{H_2O_2}^{s} = 0 \quad (4)$$

where $R^{s}_{H_2O_2}$ indicates reaction rate per (total) unit volume of liquid (kmol $m^{-3}_{tot.}$ s^{-1}). Because the hydrogen peroxide reactant is always in excess, the latter can be written as follows [6]:

$$R^{s}_{H_2O_2} = k''_{R_{H_2O_2}}(\phi_{aq}[H_2O_2]^{s})^2(\phi_{aq}[Ep]^{s}) = k'_{R_{H_2O_2}}([H_2O_2]^{s})^2[Ep]^{s} = k_{R_{H_2O_2}}[Ep]^{s} = a_s k_{Rs_{H_2O_2}}[Ep]^{s} \quad (5)$$

where $[H_2O_2]^{s}$ and $[Ep]^{s}$ are the surface concentrations of hydrogen peroxide and epoxide groups per unit volume of the aqueous phase, respectively (kmol m^{-3}), ϕ_{aq} is the volume fraction of the aqueous phase, $k'_{R_{H_2O_2}}$ is a pseudo-homogeneous reaction rate, per unit (total) volume ($m^{6}_{tot.}$ $kmol^{-2}$ s^{-1}), $k_{R_{H_2O_2}}$ is a pseudo-first order reaction rate equal to $k_{Rs_{H_2O_2}}$ times a_s (s^{-1}) and $k_{Rs_{H_2O_2}}$ is the reaction rate constant per unit of external surface of the IER catalyst ($m^{3}_{tot.}$ m^{-2}_{IER} s^{-1} = m s^{-1}).

Eq. (5) is founded on the following findings, which hold for the complete range of experimental conditions [6]: (a) the partition of hydrogen peroxide between the aqueous and gel phases is nearly constant, and (b) the observable evolution of the reaction rate using Amberlite IR-120 indicates a behavior which excludes the saturation of the catalyst surface with the organic compound and suggests – on the contrary – that it is appropriate to postulate its linear partition between the aqueous and gel phases.

Hence:

$$-\frac{1}{V}\frac{dn^{org}_{Ep}}{dt} = J^{org}_{Ep}a = J^{aq}_{Ep}a = J^{s}_{Ep}a_s = R^{s}_{H_2O_2} \quad (6)$$

Using mass transfer coefficients on each of the fluid interfaces (and recalling that the organic phase is dispersed into the aqueous phase), the former expression can be cast into the following:

$$-\phi_{org}\frac{d[Ep]^{org}}{dt} = k_{d_{Ep}}([Ep]^{org} - [Ep]^{i,org})a = k_{c_{Ep}}([Ep]^{i,aq} - [Ep]^{aq})a = k_{s_{Ep}}([Ep]^{aq} - [Ep]^{s})a_s = a_s k_{Rs_{H_2O_2}}[Ep]^{s} \quad (7)$$

where $[Ep]^{i,org}$ and $[Ep]^{i,aq}$ are the interfacial concentrations of the epoxide groups on the organic and the aqueous sides, respectively (kmol m^{-3}), $k_{c_{Ep}}$ is the mass transfer coefficient in the continuous phase (m s^{-1}), $k_{d_{Ep}}$ the mass transfer coefficient in the disperse phase (m s^{-1}) and $k_{s_{Ep}}$ the mass transfer coefficient on the fluid side of the liquid–solid interface (m s^{-1}).

Eliminating from Eq. (7) the (unknown) interfacial concentrations of the epoxide, by means of its distribution constant ($m_{Ep} = [Ep]^{i,aq}/[Ep]^{i,org}$, that is, the interface is always at equilibrium) one finally gets:

$$-\phi_{org}\frac{d[Ep]^{org}}{dt} = [Ep]^{org}\left\{\frac{1}{a}\left[\frac{1}{k_{dEp}} + \frac{1}{(m_{ep}k_{cEp})}\right] + \frac{1}{a_s}\left[\frac{1}{(m_{Ep}k_{sEp})} + \frac{1}{(m_{Ep}k_{Rs_{H_2O_2}})}\right]\right\}^{-1} \quad (8)$$

$$\frac{d[Ep]^{org}}{dt} = k_{obs_{H_2O_2}}[Ep]^{org} \quad (9)$$

where the inverse of $k_{obs_{H_2O_2}}$ represents the 'total resistance' due to transport and reactivity; that is:

$$\frac{1}{k_{obs}} = \phi_{org}\left\{\frac{1}{a}\left[\frac{1}{k_{dEp}} + \frac{1}{(m_{Ep}k_{cEp})}\right] + \frac{1}{a_s}\left[\frac{1}{(m_{Ep}k_{sEp})} + \frac{1}{(m_{Ep}k_{Rs_{H_2O_2}})}\right]\right\} \quad (10)$$

To model adequately the reactivity on this heterogeneous liquid–liquid–solid system the diffusion coefficient (Appendix B), the specific area of the aqueous–organic interface (Appendix C), the mass-transfer coefficients in the liquid–liquid subsystem, for the continuous and the disperse phases (Appendix D), the mass-transfer coefficients at the liquid–solid interface

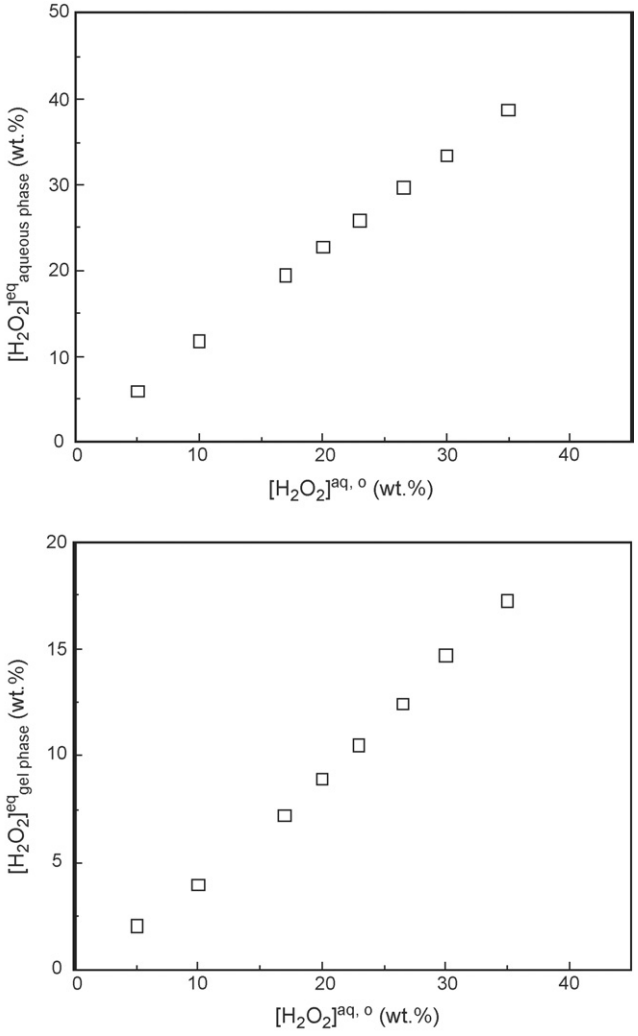

Fig. 2. Relationship between the initial concentration of hydrogen peroxide in the aqueous phase (prior to the contact with the IER) and its equilibrium concentration in both, the aqueous and 'polymer' phases. (Conditions: 333 K, H_2O_2(aq)/ESBO volume ratio = 25/15, 2.83 wt.% -dry basis- of IER with respect to the mass of ESBO).

Table 4
Reaction rate constants per unit of external catalyst surface for the oxirane ring opening of epoxidized soybean oil by H_2O_2(aq), using Amberlite IR 120 ion exchange resin as solid catalyst

Run	$(ak_{dEP})^{-1} \times 10^3$(s)	$(am_{Ep}k_{cEp})^{-1} \times 10^4$(s)	$(a_s m_{Ep}k_{sEp})^{-1} \times 10^4$(s)	$(a_s m_{Ep}k_{Rs_{H_2O_2}})^{-1} \times 10^6$(s)	$k_{Rs_{H_2O_2}} \times 10^1$(m s^{-1})
1	7.50	8.52	1.82	0.29	2.28 ± 0.0132
2	6.36	7.20	1.56	0.93	7.27 ± 0.00644
3	5.04	5.76	1.27	3.66	28.3 ± 0.0414
4	6.36	7.20	3.28	0.91	7.45 ± 0.00612
5	6.36	7.20	1.92	0.95	7.07 ± 0.00513
6	6.36	7.20	5.21	0.86	6.68 ± 0.00219
7	4.86	5.22	1.46	3.01	23.3 ± 0.0319
8	4.86	5.58	1.40	3.59	27.8 ± 0.0213

(Appendix E) and the external area of the catalyst particles (Appendix F) must be calculated.

Fig. 2 (which was obtained using Musante et al.'s data [12]) depicts the initial concentration of hydrogen peroxide in the aqueous phase (that is, prior to the contact of the solution with the resin) versus its equilibrium concentration in both, aqueous and 'polymer' phases, at 333 K.

Table 4 contains the calculated values, employing Eq. (10), of the reaction rate constants per unit of external catalyst surface ($k_{Rs_{H_2O_2}}$). The different parameters were estimated as is detailed in Appendices B–F, while k_{obs} was obtained from the experimental results themselves, using Eq. (9) (see also Ref. [6]). These values clearly indicate that in this case the system is under chemical control, as the terms involving mass transfer resistances (see Eq. (10)) are far less important than the intrinsic resistance of the chemical reaction.

Also, upon comparison of the values of the observable kinetic rate constant which takes into account just the external surface of the resin, k_{s3}, resulting from a pseudohomogeneous model [6], with those of $k_{Rs_{H_2O_2}}$ calculated here, it can be appreciated that the last ones are up to three orders of magnitude higher. This certainly suggests that even under the kinetic control regime a pseudohomogeneous model is inadequate or, better asserted, unable to identify the underlying scale of surface reactivity of the process.

Using the set of nominal diameters employed, 500, 200 and 50 μm (entries 2, 4 and 5 in Table 4), adjusted to their corresponding swelled particle volumes [12], the values of $k_{Rs_{H_2O_2}}$ were practically identical, which confirms that the surface protons are responsible of the undesired attack on the oxirane ring by hydrogen peroxide.

Finally, the impact of the amount of resin added to the system was considered. When the mass of catalyst was triplicated (nominal diameter 500 μm, entries 2 and 6 in Table 4) the reactivity ratio between these two runs was almost three as well, but $k_{Rs_{H_2O_2}}(8.49\,\text{wt.\%})/k_{Rs_{H_2O_2}}(2.83\,\text{wt.\%}) = 0.92$. This confirms, again, the direct proportionality between the increase of the external surface sites and the observed reactivity, as seen in the previous test.

3.2. Oxirane ring opening with solvated acetic acid

This reacting system is far more complex because, besides the degradation of the oxirane ring onto the catalyst surface, the carboxylic acid can attack the epoxide in the bulk of the organic and the aqueous phases. Once again, the hydrolysis reaction is negligible in comparison with the attack by acetic acid, which is in excess in all the phases [7]. Table 3 shows the different experimental conditions under which the ring-opening with AA(aq), in the presence of Amberlite IR-120 was analyzed, and the final conversions after given elapsed times.

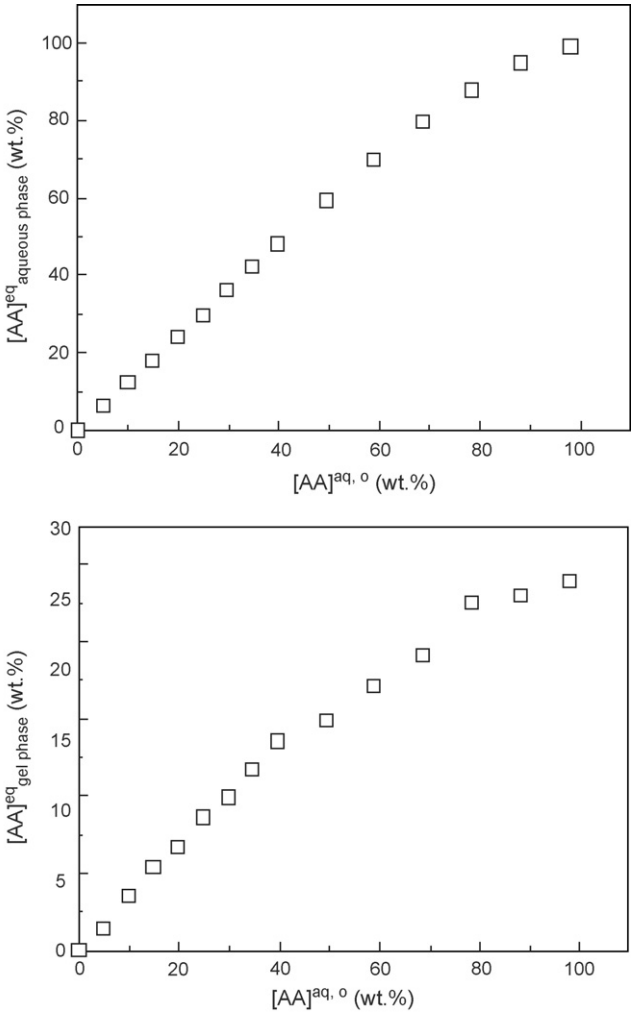

Fig. 3. Relationship between the initial (prior to the contact) vs. the equilibrium concentrations of acetic acid in the aqueous and the gel (Amberlite IR-120) phases. (Conditions: 333 K, AA(aq)/ESBO volume ratio = 25/15, 2.83 wt.% – dry basis – of IER with respect to the mass of ESBO).

Table 5
Reaction rate constants for the oxirane ring opening of epoxidized soybean oil by water-solvated acetic acid, using Amberlite IR 120 ion exchange resin as solid catalyst

Run	$k'^{org}_{R_{AA}}$ ($m^6\,kmol^{-2}\,s^{-1}$)[a]	$k'^{aq}_{R_{AA}}$ ($m^6\,kmol^{-2}\,s^{-1}$)[a]	k_{Rs} ($m\,s^{-1}$)
1	4.68×10^{-7}	6.37×10^{-3}	$9.32 \pm 0.0951 \times 10^{2}$
2	2.27×10^{-7}	3.52×10^{-3}	$3.70 \pm 0.0612 \times 10^{2}$
3	8.68×10^{-7}	1.14×10^{-3}	$29.7 \pm 0.0411 \times 10^{2}$
4	4.68×10^{-7}	6.63×10^{-3}	$7.45 \pm 0.0367 \times 10^{2}$
5	4.68×10^{-7}	6.42×10^{-3}	$21.2 \pm 0.820 \times 10^{2}$
6	4.68×10^{-7}	6.48×10^{-3}	$85.3 \pm 0.914 \times 10^{2}$
7	4.68×10^{-7}	6.37×10^{-3}	$9.32 \pm 0.0931 \times 10^{2}$
8	4.68×10^{-7}	6.37×10^{-3}	$9.33 \pm 0.0752 \times 10^{2}$
9	4.68×10^{-7}	6.37×10^{-3}	$9.07 \pm 0.0175 \times 10^{2}$

[a] From Ref. [8].

As the reacting device is an ideal (perfectly mixed), isothermal batch reactor, using the same assumptions as with the previous reacting system and taking into account that the partition of acetic acid between the organic and aqueous phases is almost unchanged with the extent of reaction, the mass balance for the epoxide groups in the former phase is the following:

$$\frac{1}{V}\frac{dn^{org}_{Ep}}{dt} = (1-\phi_{aq})\frac{1}{V}\frac{dn^{org}_{Ep}}{dt} = -J^{org}_{Ep}a - R^{org}_{AA} \quad (11)$$

Likewise, in the aqueous phase:

$$\frac{1}{V}\frac{dn^{aq}_{Ep}}{dt} = \phi_{aq}\frac{1}{V_{aq}}\frac{dn^{aq}_{Ep}}{dt} = J^{aq}_{Ep}a - J^{s}_{Ep}a_s - R^{aq}_{AA} \quad (12)$$

The homogeneous reaction rate, in either phase, is the following [7]:

$$R^{L}_{AA} = k''^{L}_{R_{AA}}(\phi_L[AA]^L)^2(\phi_L[Ep]^L) = k'^{L}_{R_{AA}}([AA]^L)^2[Ep]^L \quad (13)$$

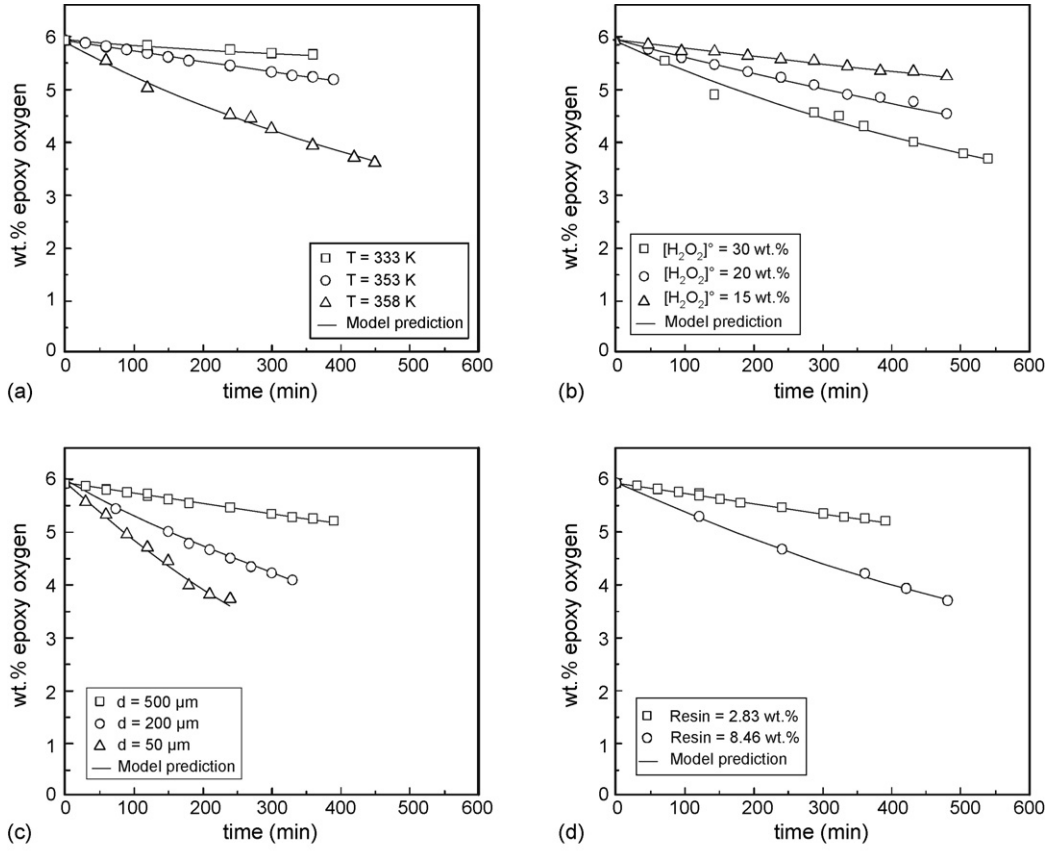

Fig. 4. Comparison between experimental data and model predictions in the oxirane ring opening of ESBO with hydrogen peroxide using Amberlite IR-120: (a) effect of temperature ($[H_2O_2]^{aq,o}$ = 30 wt.%; IR-120: d_p = 500 μm and 2.83 wt.% – dry basis – with respect to the mass of ESBO); (b) effect of the initial concentration of H_2O_2 (aq) (343 K; IR-120: d_p = 500 μm and 2.83 wt.% – dry basis – with respect to the mass of ESBO); (c) effect of resin particle diameter (343 K; $[H_2O_2]^{aq,o}$ = 30 wt.%; IR-120: 2.83 wt.% – dry basis – with respect to the mass of ESBO); and (d) effect of amount of resin introduced to the system (343 K; $[H_2O_2]^{aq,o}$ = 30 wt.%; IR-120: d_p = 500 μm). Volume ratio: 25/15; 1500 rpm. Full lines represent model predictions.

The liquid–liquid interface is at steady state, so that:

$$aJ_{\mathrm{Ep}}^{\mathrm{org}} = aJ_{\mathrm{Ep}}^{\mathrm{aq}} \tag{14}$$

Likewise, at the liquid–solid interface:

$$a_{\mathrm{s}}J_{\mathrm{Ep}}^{\mathrm{aq}} - R_{\mathrm{AA}}^{\mathrm{s}} = 0 \tag{15}$$

where $R_{\mathrm{AA}}^{\mathrm{s}}$ is the reaction rate on the catalyst surface which, expressed by unit *total* volume of liquid (kmol $m_{\mathrm{tot.}}^{-3}$ s^{-1}) can be written as:

$$R_{\mathrm{AA}}^{\mathrm{s}} = k''_{R_{\mathrm{AA}}}(\phi_{\mathrm{aq}}[\mathrm{AA}]^{\mathrm{s}})^2(\phi_{\mathrm{aq}}[\mathrm{Ep}]^{\mathrm{s}}) = k'_{R_{\mathrm{AA}}}([\mathrm{AA}]^{\mathrm{s}})^2[\mathrm{Ep}]^{\mathrm{s}} \tag{16}$$

Here, $[\mathrm{AA}]^{\mathrm{s}}$ and $[\mathrm{Ep}]^{\mathrm{s}}$ are the concentrations of acetic acid and epoxide groups on the catalyst surface, per unit volume of aqueous phase (kmol m^{-3}), respectively, and $k'_{R_{\mathrm{AA}}}$ is a pseudohomogeneous reaction rate constant per unit total volume ($m_{\mathrm{tot.}}^{6}$ kmol^{-2} s^{-1}). Because the carboxylic acid is always in excess, Eq. (16) can be re-written as:

$$R_{\mathrm{AA}}^{\mathrm{s}} = k_{R_{\mathrm{AA}}}[\mathrm{Ep}]^{\mathrm{s}} = a_{\mathrm{s}}k_{\mathrm{Rs}_{\mathrm{AA}}}[\mathrm{Ep}]^{\mathrm{s}} \tag{17}$$

where $k_{R_{\mathrm{AA}}}$ is a pseudo-first order reaction rate constant (s^{-1}) and $k_{\mathrm{Rs}_{\mathrm{AA}}}$ ($m_{\mathrm{tot.}}^{3}$ m_{IER}^{2} s^{-1} = m s^{-1}) is the reaction rate constant per unit of external catalyst surface.

Lastly, at the organic–aqueous interface, the following holds:

$$m_{\mathrm{Ep}} = \frac{[\mathrm{Ep}]^{\mathrm{i,aq}}}{[\mathrm{Ep}]^{\mathrm{i,org}}} \tag{18}$$

The correlations and/or criteria indicated in Appendices B–F were used to obtain adequate estimates of the model parameters, namely: mass transfer coefficients in the organic (disperse) and aqueous (continuous) phases, diffusion coefficients, mean diameter and specific area of the organic droplets, mass transfer coefficient at the liquid–solid interface and external area of the catalyst particles.

As already seen in the previous section for the case of H_2O_2(aq), one has to take into account that the components of the aqueous phase (here, acetic acid and water) are distributed between this, and the gel (IER) phase. The carboxylic acid, also, partitions between the organic and the aqueous phases. To illustrate matters, Fig. 3 depicts the initial (that is, prior to the contact) versus the equilibrium concentrations of acetic acid in the aqueous and the gel (Amberlite IR-120) phases, at 333 K; the figure was obtained using literature data [12]. This piece of information was used as such, i.e., without any additional simplification, in the final system modeling.

To arrive at a kinetic rate constant expressed per unit of external catalyst surface ($k_{\mathrm{Rs}_{\mathrm{AA}}}$), the individual values of the kinetic

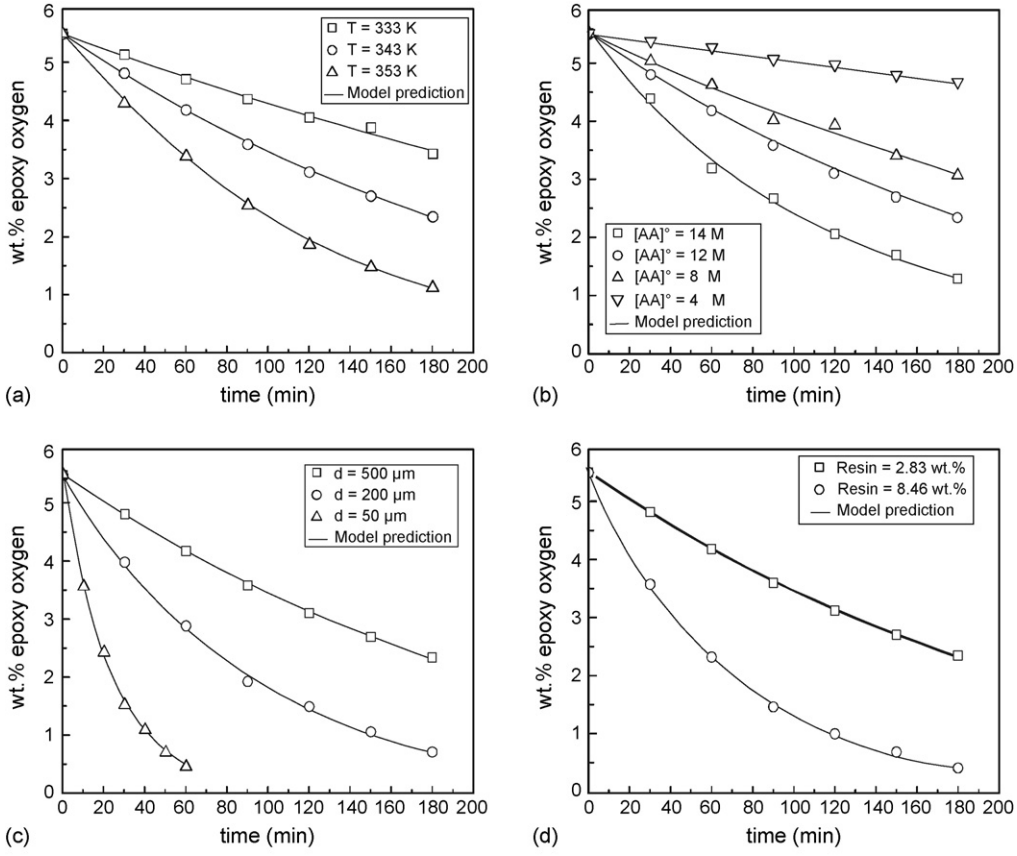

Fig. 5. Comparison between experimental data and model predictions in the oxirane ring opening of ESBO with solvated acetic acid, using Amberlite IR-120: (a) effect of temperature ($[\mathrm{AA}]^{\circ}$ = 12 M; IR-120: d_{p} = 500 μm and 2.83 wt.% – dry basis – with respect to the mass of ESBO); (b) effect of the initial concentration of acetic acid (343 K; IR-120: d_{p} = 500 μm and 2.83 wt.% – dry basis – with respect to the mass of ESBO); (c) effect of resin particle diameter (343 K; $[\mathrm{AA}]^{\mathrm{aq,o}}$ = 12 M; IR-120: 2.83 wt.% – dry basis – with respect to the mass of ESBO); and (d) effect of amount of resin introduced to the system (343 K; $[\mathrm{AA}]^{\mathrm{aq,o}}$ = 12 M; IR-120: d_p = 500 μm).Volume ratio: 25/15; 1500 rpm. Full lines represent model predictions.

rate constants of the homogeneous degradation reactions in the organic ($k'^{org}_{R_{AA}}$) and aqueous ($k'^{aq}_{R_{AA}}$) phases are needed. These values were obtained in a previous work [7] in which it was established that, if no homogeneous acidic catalyst is used, the epoxide ring opening in the bulk of either phase proceeds under the slow (kinetic) regime.

Table 5 gives values of $k'^{org}_{R_{AA}}$, $k'^{aq}_{R_{AA}}$ and $k_{Rs_{AA}}$ for the full set of experimental conditions; the latter were calculated using Eqs. (11), (12), (14), (15), (17) and (18). Being the transport parameters quite similar than in the former case (the attack on the ring by hydrogen peroxide), these results confirm that the oxirane ring opening by acetic acid on the catalyst surface proceeds under chemical control.

Using the heterogeneous model, the relative scale of the attack on the oxirane ring via the heterogeneous versus the homogeneous routes was found to be negligible both in the aqueous *and* in the organic phases, while – under the full range of experimental conditions used in this work – most of the ring-opening occurs in the gel (acidic catalyst) phase (Tables 3 and 5). At this stage it is appropriate to point out that upon using Amberlite IR-120 beads (500 μm, 2.83 wt.%, dry basis (with respect to the amount of ESBO), the *total* amount of protons brought into the system by the IER was higher than that resulting from the addition of H_2SO_4 to give pH 1 in the aqueous phase but, nevertheless, the ensuing ring-opening became far more restricted [7]. This huge difference in undesired degradation of the ESBO and, consequently, improved performance of the IER with respect to mineral acids, is entirely due to the gel-like nature of Amberlite IR-120, as it was already discussed.

Using aliquots of the crushed resin, with nominal diameters equal to 500, 200 and 50 μm, the individual values of $k_{Rs_{AA}}$ were – within the experimental error – almost equal (entries 1, 7 and 8 in Table 5). Also, upon trebling the amount of catalyst, the ratio of the corresponding surface reaction rate constants (entries 1 and 9 of same table) was: $k_{Rs_{AA}}(8.49\,\text{wt.\%})/k_{Rs_{AA}}(2.83\,\text{wt.\%}) = 0.97$, in complete agreement with our previously finding about the external surface protons being the main responsible of the epoxide groups degradation.

Finally, Figs. 4 and 5 compare the experimental results and model predictions (employing Euler's numeric method) in the oxirane ring opening of epoxidized soybean oil with H_2O_2 (aq) and solvated acetic acid used in this work. The proposed models adequately describe the concentration profiles as a function of time in both cases.

4. Conclusions

The combined results on the attack onto the oxirane ring of epoxidized vegetable oils by either hydrogen peroxide or solvated acetic acid using a heterogeneous strong acidic catalyst such as the gel-type ion exchange resin Amberlite IR-120 indicate that under 'regular' process conditions these attacks proceed under the kinetic regime; that is, they are not mass-transfer controlled.

By using a heterogeneous liquid–liquid–solid model, the reactivity on each phase was individually assessed. The study confirmed that the surface protons of the IER are the main responsibles of the deleterious degradation of the oxirane ring as, in both cases, the degradation rate was directly proportional to the available external area of the catalyst.

Certainly, whenever intrinsic kinetic rate constants are sought after, it is no longer possible to model the reacting system as pseudohomogeneous but, on the contrary, each transport and kinetic steps on each phase must be taken into account.

Acknowledgments

The authors thank ANPCyT, CONICET and UNL for their financial support.

Appendix A. Nomenclature

$[j]^L$	concentration of compound j in the L phase (kmol m^{-3})
a	interfacial area between the organic and the aqueous phases ($m^2\ m^{-3}_{tot.}$)
a_s	external area of the catalyst particles per unit total volume of the reacting system ($m^2\ m^{-3}_{tot.}$)
d^*	diameter number
d_{32}	mean Sauter diameter (m) $= (\Sigma n_i d_i^3)/(\Sigma n_i d_i^2)$
d_p	mean diameter of the catalyst particles (m)
D_a	stirrer diameter (m)
D_j	diffusion coefficient of compound j in the L phase ($m^2\ s^{-1}$)
J_j	molar flux of compound j (kmol $m^{-2}\ s^{-1}$)
k_L	mass-transfer coefficient in the L phase ($m\ s^{-1}$)
k_{Rj}	pseudo-first order reaction rate constant (s^{-1})
k'_{Rj}	pseudohomogeneous reaction rate constant, per total unit volume of the reacting system ($m^6_{tot.}$ kmol$^{-2}\ s^{-1}$)
$k_{R_{sj}}$	reaction rate constant, per unit of external surface, for compound j ($m\ s^{-1}$).
m_j	distribution constant of compound j ($[j]^{i,aq}/[j]^{i,org}$), dimensionless
M_j	molecular weight of compound j (kg $kmol^{-1}$)
n_a	stirring speed (s^{-1})
n_i	number of drops with diameter d_i of the disperse phase
n^L_j	number of moles of compound j in the L phase (kmol)
P	power dissipated by the stirrer (kg $s^{-3}\ m^{-2}$)
R	reaction rate per unit total volume of liquid (kmol $m^{-3}_{tot.}\ s^{-1}$)
T	absolute temperature (K)
V	total liquid volume (m^3)
V_j	molar volume of compound j ($m^3\ kmol^{-1}$)
V_L	volume of the L phase (m^3)
w_j	mass of compound j (kg)
W	mass of catalyst with respect to the mass of ESBO introduced in the reactor, dry basis ($kg_{IER}\ kg^{-1}_{ESBO}$)
We	Weber number $= \rho_c n_a^2 D_a^3/\sigma$
x_i	molar fraction of solvent i

Greek symbols

ψ	power number, dimensionless
σ	surface tension (N m^{-1})
ϕ_L	volume fraction of the L phase ($m^3_L\ m^{-3}_{tot.}$)

ρ density (kg m^{-3})
μ viscosity (kg m^{-1} s^{-1})

Sub and superscripts
AA acetic acid
aq aqueous phase
eq equilibrium
Ep epoxide group
EpO epoxide oxygen
L generic (organic or aqueous) phase
i, aq aqueous interface
i, org organic interface
i, s property at the catalyst surface
IER ion exchange resin
l liquid
j compound j
o initial
org organic phase
s solid
tot. total

Appendix B. Estimation of diffusion coefficients

The diffusion coefficients in the multicomponent liquid mixtures were estimated using the simple, semi-empirical model of Perkins and Geankoplis based on a modified version of the Wilke and Chang equation [13]:

$$D_{AM} = \frac{F \times 10^{-5} T}{\mu_M} \tag{B1}$$

$$F = \frac{4.67 \times 10^{-6} (\theta_M M_M)^{0.5}}{V_A^{0.6}} \tag{B2}$$

$$\theta_M M_M = \Sigma x_i \theta_i M_i \tag{B3}$$

where D_{AM} is the diffusion coefficient of solute A in the solvents mixture (m^2 s^{-1}), μ_M the viscosity of the mixture (kg m^{-1} s^{-1}), θ_M the association factor of the mixture, M_M the mean molecular mass of the mixture (kg kmol^{-1}), V_A the molar volume of solute A at its normal boiling point (m^3 kmol^{-1}), T the absolute temperature (K), x_i the molar fraction of solvent i, θ_i the association factor of solvent i and M_i is the molecular mass of solvent i (kg kmol^{-1}).

So, for example, the calculated diffusion coefficient of ESBO in the polar phase, at 343 K, in a mixture of epoxidized soybean oil-aqueous H_2O_2 (30 wt.%) is 1.25×10^{-9} m^2 s^{-1}, whereas for the system epoxidized oil-(aqueous) solvated acetic acid ([AA]$^\circ$ = 15 M) is 6.94×10^{-8} m^2 s^{-1}.

Appendix C. Estimation of the liquid–liquid (organic–aqueous) interfacial area

The interfacial area was calculated using the following expression [14,15]:

$$a = \frac{6\phi_d}{d_{32}} \tag{C1}$$

where d_{32} is the Sauter mean diameter (m), which value is equal to $(\Sigma n_i d_i^3)/(\Sigma n_i d_i^2)$ and n_i represents the number of drops with diameter d_i.

The equation used to estimate d_{32} was the following [14]:

$$\frac{d_{32}}{D_a} = \frac{A f(\phi_d)}{We^{0.6}} \tag{C2}$$

where D_a is the stirrer diameter (m), *We* the Weber number $(\rho_c n_a^2 D_a^3/\sigma)$, n_a the stirring velocity (s^{-1}), ρ_c the continuous phase density (kg m^{-3}), σ the surface tension (N m^{-1}) and A is a parameter whose value ranges between 0.04 and 0.4. The function $f(\phi_d)$ can be represented in two ways, both of which account for re-dispersion and coalescence effects. A linear function, for instance, gives:

$$f(\phi_d) = 1 + B\phi_d \tag{C3}$$

where B is a constant between 2 and 9 for redispersions in which $\phi_d < 0.2$ [14,15]. When $\phi_d > 0.3$ Eq. (C3) is no longer valid, and therefore another function must be used. For example, Delichatsios and Probstein [16] have recommended, instead, the following:

$$f(\phi_d) = \left[\frac{\ln(c_2 + c_3\phi_d)}{\ln c_2}\right]^{-3/5} \tag{C4}$$

where c_2 (=0.011) and c_3 are constants. The latter constant is proportional to the ratio between the coalescence and dispersion coefficients, whose value must be empirically determined, and differs from one system to another (such value is always close to 1.0).

Even though our experimental device had a 2-blade stirrer ($D_a = 1.00 \times 10^{-2}$ m), our calculations of d_{32} were made using the former authors' data (where a 4.00×10^{-2} m turbine was used instead), because for this small-reactor scale no significant differences in performance exist among stirrers [6,7]. According to this, then, the power number in our particular case is equal to 5. Eq. (C2) was used to estimate the Sauter mean diameter. The linear function given by Eq. (C3) was used for the ESBO-solvated acetic acid system, and Eq. (C4) for the other system (ESBO-hydrogen peroxide). Using these d_{32} values the interfacial areas were determined, in turn, through Eq. (C1).

As a way of example, the estimated values of the interfacial area between the organic and the aqueous phases, at 343 K in the mixture of ESBO and aqueous H_2O_2 (30 wt.%) is 1.34 m^2 m^{-3} and for the system ESBO-(aqueous) solvated acetic acid ([AA]$^\circ$ = 15 M) is 12.56 m^2 m^{-3}.

Appendix D. Estimation of mass transfer coefficients in the liquid–liquid systems

D.1. Mass transfer coefficients in the continuous phase

The correlation of Calderbank and Moo-Young [17] was used in this work:

$$k_c = 1.3 \times 10^{-3} \left[\frac{P\mu_c}{V_c \rho_c^2}\right]^{0.25} \left[\frac{\mu_c}{\rho_c D_A}\right]^{-0.67} \tag{D3}$$

$$P = \psi \rho_m n_a^3 D_a^5 \quad \text{(D4)}$$

where P is the power dissipated by the agitator ($\mathrm{kg\,(s^3\,m^2)^{-1}}$) and ψ is the power number.

The values of dissipated power (Eq. (D4)) and the mass transfer coefficients in the continuous phase (Eq. (D3)) for the different liquid–liquid systems were calculated using $\psi = 5$ for each experimental temperature. To exemplify matters: at 343 K the estimated value of k_c in the mixture of ESBO and aqueous H_2O_2 (30 wt.%) is $6.50 \times 10^{-5}\ \mathrm{m\,s^{-1}}$ and for the system ESBO-(aqueous) solvated acetic acid ($[AA]^\circ = 15$ M) is $4.15 \times 10^{-5}\ \mathrm{m\,s^{-1}}$.

D.2. Mass transfer coefficients in the disperse phase

The value of the mass transfer coefficient in the disperse phase depends on the drop behavior; mostly upon whether the drop is rigid or not. To be able to evaluate the latter, the diameter number (d^*) must be calculated [15]:

$$d^* = d_{32}\left[\frac{\mu_c^2}{\rho_c g \Delta\rho}\right]^{-1/3} \quad \text{(D5)}$$

where d^* must be less than 10 for the drops to be considered as rigid spheres.

For a rigid sphere, Treybal [18] gives the following relationships:

$$N_{sh} = \frac{2\pi^2}{3} \quad \text{(D6)}$$

$$N_{sh} = \frac{k_d d_{32}}{D_A} \quad \text{(D7)}$$

Considering both, Eqs. (D6) and (D7):

$$k_d = \frac{2\pi^2 D_A}{3 d_{32}} \quad \text{(D8)}$$

As the calculated values of d^* were less than 10, the organic phase drops can be taken as rigid spheres. Thus, k_d values were calculated using Eq. (D8). At 343 K, for example, the estimated value for k_d in the mixture of ESBO and aqueous H_2O_2 (30 wt.%) was $4.92 \times 10^{-4}\ \mathrm{m\,s^{-1}}$ and for the system ESBO-(aqueous) solvated acetic acid ($[AA]^\circ = 15$ M) it was $5.98 \times 10^{-5}\ \mathrm{m\,s^{-1}}$.

Appendix E. Estimation of the mass transfer coefficients at the liquid–solid interface

These mass transfer coefficients were calculated using the Calderbank and Moo-Young correlation for liquid–solid interfaces [17,19]:

$$k_s d_p D^{-1} = 2 + 0.31\, D^{5/3}\left[\frac{(\rho_{IER} - \rho_1)}{\mu_1}\right]^{1/3} \quad \text{(E.1)}$$

where k_s is the liquid–solid mass transfer coefficient ($\mathrm{m\,s^{-1}}$), d_p is the mean diameter of the solid particles (m) and g is the gravity acceleration ($\mathrm{m\,s^{-2}}$).

The calculated value of k_s at 343 K in the system constituted by the ESBO-aqueous H_2O_2 (30 wt.%)-IER (2.83 wt.%; d_p (swollen) = 682 μm) was $5.03 \times 10^{-5}\ \mathrm{m\,s^{-1}}$. For the system ESBO-(aqueous) solvated acetic acid ($[AA]^{eq}_{\text{polymer phase}} = 3.65$ M)-IER (2.83 wt.%; d_p (swollen) = 682 μm), said value was $2.83 \times 10^{-5}\ \mathrm{m\,s^{-1}}$.

Appendix F. External area of the catalyst particles per unit total volume

The external area of the IER particles per unit (total) volume, a_s ($\mathrm{m^2_{IER}\,m^{-3}_{tot.}}$), was calculated using the following equation [19]:

$$a_s = W\rho_{ESBO}(1 - \phi_{aq})\frac{6}{d_p}\frac{1}{\rho_{IER}} \quad \text{(F.1)}$$

where W is the mass of resin (dry basis) with respect to the mass of ESBO introduced in the reactor ($\mathrm{kg_{IER}\,kg^{-1}_{ESBO}}$). The a_s values were estimated considering the final diameters of the swollen resin. So, for example, using 2.83 wt.% IER with d_p (swollen) = 682 μm the external area of the resin particles in the system ESBO-aqueous H_2O_2 (30 wt.%)-IER (2.83 wt.%; d_p (swollen) = 682 μm) was $47.64\ \mathrm{m^2\,m^{-3}_{tot.}}$, at 343 K. For the system ESBO-(aqueous) solvated acetic acid ($[AA]^{eq}_{[\text{polymer phase}]} = 3.65$ M)-IER (2.83 wt.%; $d_p = 682$ μm) said value was $30.89\ \mathrm{m^2\,m^{-3}_{tot.}}$, also at 343 K.

References

[1] B. Rangarajan, A. Havey, E.A. Grulke, P.D. Culnan, Kinetic parameters of a two-phase model for in-situ epoxidation of soybean oil, J. Am. Oil Chem. Soc. 72 (10) (1995) 1161–1169.

[2] J. La Scala, R.P. Wool, Effect of FA composition on epoxidation kinetics of TAG, J. Am. Oil Chem. Soc. 79 (4) (2002) 373–378.

[3] S. Sinadinović-Fišer, M. Janković, Z.S. Petrović, Kinetics of in-situ epoxidation of soybean oil in bulk catalyzed by ion exchange resin, J. Am. Oil Chem. Soc. 78 (7) (2001) 725–731.

[4] Z.S. Petrović, A. Zlatanić, C.C. Lava, S. Sinadinović-Fišer, Epoxidation of soybean oil in toluene with peroxoacetic and peroxoformic acids. Kinetics and side reactions, Eur. J. Lipid Sci. Technol. 104 (2002) 293–299.

[5] L.H. Gan, S.H. Goh, K.S. Ooi, Kinetic studies of epoxidation and oxirane cleavage of palm olein methyl esters, J. Am. Oil Chem. Soc. 69 (4) (1992) 347–351.

[6] A. Campanella, M.A. Baltanás, Degradation of the oxirane ring of epoxidized vegetable oils with hydrogen peroxide using an ion exchange resin, Catal. Today 107–108 (2005) 208–214.

[7] A. Campanella, M.A. Baltanás, Degradation of the oxirane ring of epoxidized vegetable oils with solvated acetic acid using cation-exchange resins, Eur. J. Lipid Sci. Technol. 106 (2004) 524–530.

[8] A. Campanella, Selective Catalytic Epoxidation of Vegetable Oils in Multiphase Systems, Doctoral Dissertation, Universidad Nacional del Litoral, Argentina, 2005.

[9] Official and Recommended Practices of the American Oil Chemists' Society, fifth ed., AOCS Press, Champaign, IL, 1997.

[10] H. Sales, R. Cesquini, S. Sato, D. Mandelli, U. Schuchardt, Epoxidation of soybean oil catalysed by CH_3ReO_3/H_2O_2, Stud. Surf. Sci. Catal. 130 (2000) 1661–1665.

[11] A. Campanella, M.A. Baltanás, Degradation of the oxirane ring of epoxidized vegetable oils in liquid–liquid systems: I. Hydrolysis and attack by H_2O_2, Lat. Am. Appl. Res. 35 (2005) 205–210.

[12] R.L. Musante, R.J. Grau, M.A. Baltanás, Kinetic of liquid-phase reactions catalyzed by acidic resins: the formation of peracetic acid for vegetable oil epoxidation, Appl. Catal. A: Gen. 197 (2000) 165–173.
[13] L.R. Perkins, C.J. Geankoplis, Molecular diffusion in a ternary liquid system with the diffusing component dilute, Chem. Eng. Sci. 24 (1969) 1035–1042.
[14] J.M. Zaldívar, E. Molga, M.A. Alós, H. Hernández, K.R. Westerterp, Aromatic nitrations by mixed acid fast liquid–liquid reaction regime, Chem. Eng. Process. 35 (1996) 91–105.
[15] B.A.A. van Woezik, K.R. Westerterp, Measurement of interfacial areas with the chemical method for a system with alternating dispersed phases, Chem. Eng. Process. 39 (2000) 299–314.
[16] M.A. Delichatsios, R.F. Probstein, The effect of coalescence on the average drop size in liquid–liquid dispersions, Ind. Eng. Chem. Fundam. 15 (2) (1976) 134–138.
[17] P.H. Calderbank, M.B. Moo-Young, The continuous phase heat and mass-transfer properties of dispersions, Chem. Eng. Sci. 16 (1/2) (1961) 39–54.
[18] R.E. Treybal, Liquid Extraction, second ed., McGraw-Hill, New York, NY, 1963.
[19] H.J.L. Cantero, Analysis of the Modeling of a Turbulent Tube Reactor for Selective Hydrogenation of Vegetable Oils, Doctoral Dissertation, Universidad Nacional del Litoral, Argentina, 1993.
[20] R.C. Reid, J.M. Prausnitz y, T.K. Sherwood, The Properties of Gases and Liquids, third ed., Mc Graw-Hill, New York, NY, 1977.